simple as possible, such as using immunochromatographic test strips that are available for the detection of influenza infections. Among several candidates for diagnostic markers, we examined soluble Fas ligand (sFasL) and found that it is elevated in the sera of patients with SJS/TEN in the early stage, before mucocutaneous erosions appear.[2,3] It would be very useful to be able to predict the occurrence of SJS/TEN, but sFasL serum levels are too low (cut off: 100 pg/mL) for use in a rapid diagnostic device.

Chung et al[4] recently reported that granulysin is highly expressed in blisters of patients with SJS/TEN. We found that both serum granulysin and sFasL are higher in patients with early-stage SJS/TEN than in patients with ODSRs.[5] Serum levels of granulysin are 100 times higher (cut off: 10 ng/mL) than those of sFasL. Based on these observations, we developed a rapid immunochromatographic assay for the detection of high-level serum granulysin to diagnose and predict the early stage of SJS/TEN.

CAPSULE SUMMARY

- Drug reactions sometimes start with edematous papules, and it may be difficult to distinguish life-threatening drug reactions from ordinary drug reactions early in their course.
- We recently found that serum granulysin levels are increased in patients who later develop Stevens-Johnson syndrome or toxic epidermal necrolysis.
- We report a novel immunochromatographic assay to detect high levels of serum granulysin. With this test, we can predict whether patients with nonspecific edematous papules will develop severe drug eruptions.

METHODS

Patients

SJS refers to cases with mucosal erosions and epidermal detachment of less than 10% of the body surface area, and TEN refers to those with more than 30% involvement. Disease onset in patients with SJS/TEN was defined as the day when the mucocutaneous or ocular lesion first eroded or ulcerated (day 1).[3] From multiple Japanese institutions, we obtained serum samples from 35 patients with SJS/TEN.[3] Of these, we investigated 5 patients whose sera had been collected before the diagnosis of SJS/TEN (day −2 to −4). The patient information is listed in Table I. Serum samples from patients with ODSRs (n = 24) and healthy volunteers (n = 31) were also analyzed. Informed consent was obtained from all patients, and the procedures were approved by the Ethical Committee of the Hokkaido University Graduate School of Medicine, Sapporo, Japan.

Immunochromatographic assay

In the immunochromatographic test, a murine monoclonal antibody specific to human granulysin (RB1, MBL, Nagoya, Japan) was conjugated with microparticles and then placed on the glass membrane area of the test device in a dry state. Another granulysin monoclonal antibody (RC8, MBL) was immobilized on a nitrocellulose membrane to form a result line. Likewise, a control line was created by the immobilization of antimouse IgG. The granulysin in the serum sample specifically bound to the microparticles via RB1 and comigrated upward until the granulysin was sandwiched with the immobilized RC8, revealing a visible result line. The entire test procedure was completed within 15 minutes.

Enzyme-linked immunosorbent assay

The granulysin concentrations of the serum samples were measured with a sandwich-enzyme-linked immunosorbent assay as previously described.[6,7] In brief, 96-well flat-bottomed plates were coated with 5 mg/mL of RB1 antibody and stored overnight at 4°C. The plates were then washed and blocked with phosphate-buffered saline containing 0.1% Tween-20 (washing buffer) and blocked with 10% fetal bovine serum in washing buffer at room temperature for 2 hours. The samples and standards (recombinant granulysin, R&D Systems, Minneapolis, MN) were incubated for 2 hours at room temperature. Then they were reacted with 0.1 mg/mL of biotinylated RC8 antibody for 1 hour. The plates were then treated with 0.2 mg/mL of horseradish-peroxidase-conjugated streptavidin (Roche Diagnostics, Basel, Switzerland) for 30 minutes at room temperature. The plates were incubated with tetramethylbenzidine substrate (Sigma, St Louis, MO) for 30 minutes at room temperature, and then 1 mol/L sulfuric acid was added. The optical density was measured at 450 nm using a microplate reader (Mithras LB940, Berthold Technologies, Thoiry, France).

RESULTS

We first applied diluted recombinant human granulysin protein to the immunochromatographic test strips, to confirm the threshold and reliability of the assay. Approximately 10 ng/mL of sample yielded a result line, and 3 repeated investigations brought the same results (Fig 1, *A*).

Table I. Patient information

Patient No.	Age, y	Sex	Diagnosis	Affected skin area	Causative drug	Serum granulysin (d)
1	17	M	SJS	20%	Carbamazepine	52.1 (−3)
2	66	F	TEN	70%	Imatinib	14.2 (−3)
3	27	F	SJS	<10%	Unknown	42.2 (−4)
4	80	M	SJS	5%	Phenytoin	12.9 (−2)
5	25	F	SJS	Only mucosal lesions	Unknown	2.7 (−2)

F, Female; *M*, male; *SJS*, Stevens-Johnson syndrome; *TEN*, toxic epidermal necrolysis.

Based on this observation, we then applied serum samples to detect the elevated granulysin levels. Four of 5 SJS/TEN samples showed positive results (Fig 1, *B*). All the positive samples had elevated granulysin as detected by enzyme-linked immunosorbent assay analysis (30.35 ± 9.91 ng/mL, average ± SEM). The only sample with a negative result had granulysin at the normal level of 2.7 ng/mL. Conversely, one in 24 ODSRs samples and none of 31 healthy volunteers showed positive bands in this immunochromatographic assay. The test showed a sensitivity of 80% and a specificity of 95.8% for SJS/TEN versus ODSRs. The results of the immunochromatographic test correlated closely with early diagnosis for SJS/TEN ($P = 1.02 \times 10^{-3}$, analyzed by Fisher exact probability test).

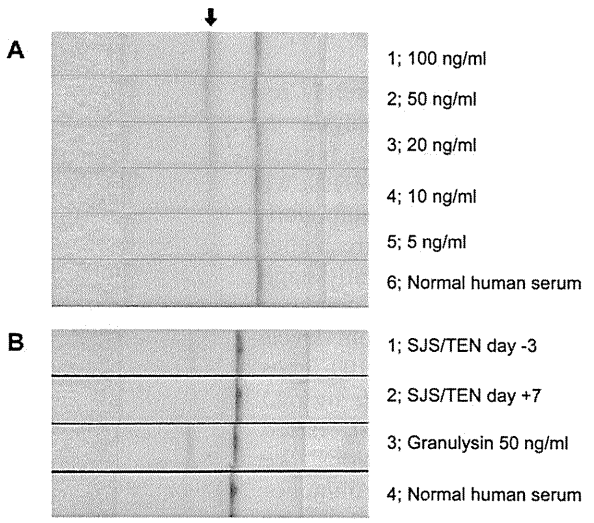

Fig 1. A, Immunochromatographic test strip detects elevated granulysin. *1 to 5*, Diluted recombinant granulysin is applied. *6*, Normal human serum as negative control (1.4 ng/mL). Positive results are shown as a band (indicated by the arrow). Approximately 10 ng/mL of granulysin is considered a positive result. **B**, Detection of serum granulysin by immunochromatographic assay. *1*, Serum taken from patient 1 with early Stevens-Johnson syndrome (*SJS*)/toxic epidermal necrolysis (*TEN*) 3 days before blister formation. Although patient showed only edematous erythema and papules without mucosal manifestations, serum granulysin was 52.1 ng/mL. *2*, Seven days after blister formation in same patient with SJS/TEN. No bands are observed, and serum granulysin has decreased to 5.7 ng/mL. *3*, Recombinant human granulysin as positive control. *4*, Normal human serum as negative control (3.5 ng/mL).

DISCUSSION

We succeeded in developing a rapid immunochromatographic test for the detection of high-level serum granulysin that puts our previous findings to practical use. Although 20% of the cases could be missed, it would be a useful adjunct in diagnosing SJS/TEN. It would not be necessary for every morbilliform drug eruption. We suggest that the test be applied when clinical findings hinting at SJS/TEN, such as target lesions, are seen. However, two biopsies should be done as soon as SJS/TEN are suspected, for hematoxylin-eosin processing and immediate frozen sections, in order to look for necrotic keratinocytes, which is another sensitive test.[8] If the results of either method are negative, careful daily and hourly monitoring of the patient for a few days should take place. Furthermore, to assess the severity of illness and to predict mortality, we should use the mathematical tool called SCORTEN that has been developed.[9]

Granulysin, a member of the saposin-like protein family of lipid-binding proteins, exhibits potent cytotoxicity against a broad panel of microbial targets, including tumor cells, transplanted cells, bacteria, fungi, and parasites, damaging negatively charged cell membranes.[10] Granulysin plays important roles in host defense against pathogens, and it induces apoptosis of target cells in a mechanism involving caspases and other pathways.[11] Chung et al[4] reported that granulysin was identified as the most highly expressed cytotoxic molecule in blisters of patients with SJS/TEN. Very recently, we showed that granulysin levels of sera from patients with SJS/TEN are significantly elevated before the development of skin detachment or mucosal lesions.[5] The elevated serum granulysin levels decrease rapidly within 5 days after disease onset. This pattern is similar to that

observed with sFasL.[3] When granulysin levels for patients with SJS/TEN in the early stage were compared with those levels for patients with ODSRs and healthy control subjects, the differences were statistically significant.[5]

This novel test enables the early diagnosis of SJS/TEN in patients with cutaneous adverse drug reactions that are otherwise indistinguishable from ODSRs.

REFERENCES

1. Roujeau JC, Kelly JP, Naldi L, Rzany B, Stern RS, Anderson T, et al. Medication use and the risk of Stevens-Johnson syndrome or toxic epidermal necrolysis. N Engl J Med 1995;333:1600-7.
2. Abe R, Shimizu T, Shibaki A, Nakamura H, Watanabe H, Shimizu H. Toxic epidermal necrolysis and Stevens-Johnson syndrome are induced by soluble Fas ligand. Am J Pathol 2003;162:1515-20.
3. Murata J, Abe R, Shimizu H. Increased soluble Fas ligand levels in patients with Stevens-Johnson syndrome and toxic epidermal necrolysis preceding skin detachment. J Allergy Clin Immunol 2008;122:992-1000.
4. Chung WH, Hung SI, Yang JY, Su SC, Huang SP, Wei CY, et al. Granulysin is a key mediator for disseminated keratinocyte death in Stevens-Johnson syndrome and toxic epidermal necrolysis. Nat Med 2008;14:1343-50.
5. Abe R, Yoshioka N, Murata J, Fujita Y, Shimizu H. Granulysin as a marker for early diagnosis of the Stevens-Johnson syndrome. Ann Intern Med 2009;151:514-5.
6. Ogawa K, Takamori Y, Suzuki K, Nagasawa M, Takano S, Kasahara Y, et al. Granulysin in human serum as a marker of cell-mediated immunity. Eur J Immunol 2003;33:1925-33.
7. Saigusa S, Ichikura T, Tsujimoto H, Sugasawa H, Majima T, Kawarabayashi N, et al. Serum granulysin level as a novel prognostic marker in patients with gastric carcinoma. J Gastroenterol Hepatol 2007;22:1322-7.
8. Pereira FA, Mudgil AV, Rosmarin DM. Toxic epidermal necrolysis. J Am Acad Dermatol 2007;56:181-200.
9. Bastuji-Garin S, Fouchard N, Bertocchi M, Roujeau JC, Revuz J, Wolkenstein P. SCORTEN: a severity-of-illness score for toxic epidermal necrolysis. J Invest Dermatol 2000;115:149-53.
10. Kaspar AA, Okada S, Kumar J, Poulain FR, Drouvalakis KA, Kelekar A, et al. A distinct pathway of cell-mediated apoptosis initiated by granulysin. J Immunol 2001;167:350-6.
11. Clayberger C, Krensky AM. Granulysin. Curr Opin Immunol 2003;15:560-5.

Special Issue "Epithelial regeneration in inflammatory diseases"

Mini Review

Regenerative medicine for severe congenital skin disorders: restoration of deficient skin component proteins by stem cell therapy

Yasuyuki Fujita*, Riichiro Abe, Wataru Nishie and Hiroshi Shimizu

Department of Dermatology, Hokkaido University Graduate School of Medicine, Sapporo, Japan

Some congenital skin disorders lacking structure proteins in the basement membrane zone carry severe prognosis because of severe erosion and skin dysfunction on the whole body. So far, several therapeutic strategies have been emerging for such disorders: 1. gene therapies, 2. protein therapies and 3. cell therapies. Cell therapies have a potential to affect skin systemically, and stem cell transplantation is one of the most hopeful candidates for treating severe congenital skin disorders such as epidermolysis bullosa, from a perspective of transdifferentiation and re-programming of stem cells. We review here the recent strategies and progress of stem cell transplantation for epidermolysis bullosa.

Rec./Acc.4/11/2011

*Correspondence should be addressed to:
Yasuyuki Fujita, Department of Dermatology, Hokkaido University Graduate School of Medicine, North 15 West 7, Kita-ku, Sapporo 060-8638, Japan. Tel: +81-11-706-7387 Fax: +81-11-706-7820 E-mail: yfujita@med.hokudai.ac.jp

Key words:
basement membrane zone, bone marrow transplantation, epidermolysis bullosa, stem cell therapy, type XVII collagen

Introduction

The skin is the human body's largest organ and accounts for approximately 16% of an adult's body weight. Several critical roles owe to the skin, including moderation of body temperature, prevention from electrolyte loss and protection from physical stimuli. In order to resist mechanical stress, the skin has complicated structures connecting epidermis and dermis, called basement membrane zone (BMZ) or dermal-epidermal junction. The BMZ consists of more than 30 structure proteins to strengthen the adhesion (Fig. 1)[1], and one defect of these proteins by congenital abnormality or acquired autoimmunity cause skin fragility and blister formation immediately after mild mechanical stimuli. Blistering on the whole body extremely worsens the quality-of life and even causes death due to severe water loss and infections.

Epidermolysis bullosa

One important example on the importance of BMZ proteins is epidermolysis bullosa (EB). EB comprises a group of inherited disorders in which the patient's epidermis can exhibit skin fragility caused by genetic abnormalities of a BMZ protein[2]. From the location of causative BMZ protein, EB is classified roughly into 3 categories: EB simplex (EBS), junctional EB (JEB) and dystrophic EB (DEB). Worldwide approximately 50 EB cases arise per a million live births and 92% accounts for EBS which is caused by cytokeratin 5/14 mutation with autosomal dominant inheritance[2]. Clinical manifestations vary broadly, from occasional mild erosion on the extremities to severe ulcers on the whole body or even stillbirth in Herlitz JEB and EBS/JEB with pyloric atresia. In recessive DEB, the most frequently recognized subtype in Japan, defect of type VII collagen (COL7) causes recurrent, deep erosions and ulcers on the extremities which results in mitten deformities and squamous cell carcinoma.

Emerging novel strategies for EB treatment

Most prevalent treatments for EB patients are skin protective care, wound dressing agents and antibiotics against local infections. There have been no established and fundamental treatments because EB arises from gene mutations of keratinocytes and fibroblasts on the whole body. However, several novel strategies have been emerging for EB treatment recently: 1. gene therapies, 2. protein therapies and 3. cell therapies.

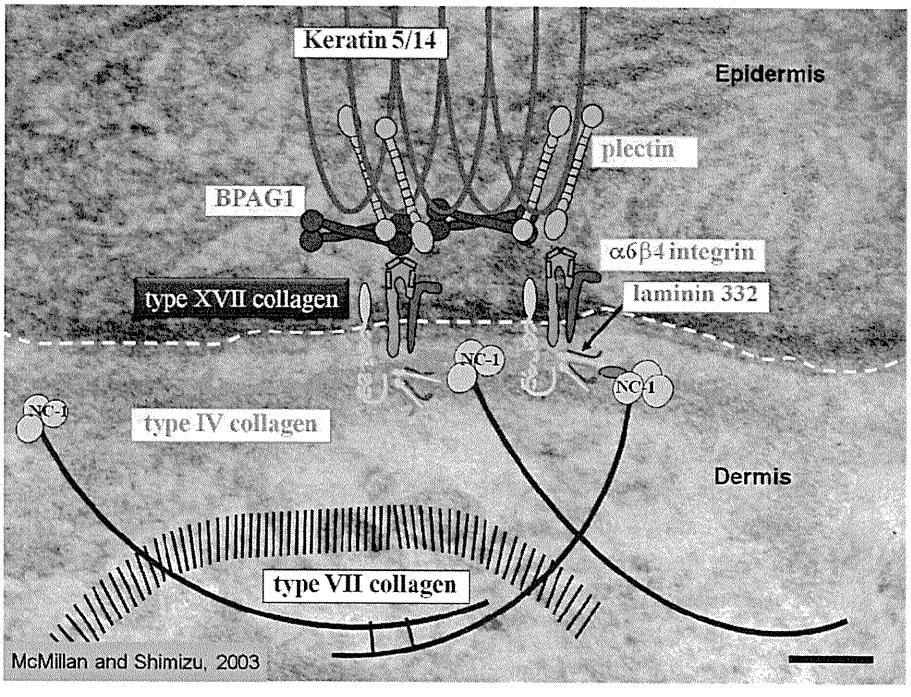

Fig. 1
Structure of basal membrane zone (BMZ) in the skin[1].

Gene therapies were performed by virus-mediated normal gene transfection into autologous keratinocytes, followed by cell culture to form epidermal sheet and grafting into the patients' skin. Such *ex vivo* gene-treated cultured autografting, reported by Mavilio *et al.*, is a promising therapeutic approach for junctional EB[3]. One of the merits of gene-mediated therapies is that autologous cells are fundamentally accepted without rejection response, except for the risk of immunoreactivity against the restored protein. Conversely, its effects are limited to the area of grafting and might be insufficient for systemic involvement of EB. Furthermore, the ethical and safety problems of using retroviruses for gene correction still exist[4]. Autologous induced pluripotent stem (iPS) cells are another source for gene therapies, since high proliferation potential provide enough number of differentiated cells without invasive techniques[5]. Successful treatment of sickle cell anemia model mice was recently reported by utilizing gene-corrected hematopoietic cell transplantation from autologous iPS cells[6]. Tolar *et al.* succeeded in the generation of autologous iPS cells from recessive DEB patient, which indicates that iPS-mediated therapies are theoretically possible by generation of epidermal/dermal sheets and hematopoietic stem cell transplantation[7]. However, ethical problems still lie on autologous iPS cells for the treatment of EB since gene correction by transfection is essential.

Conversely, few reports have been published as to *in vivo* gene therapies for EB[8]. As one candidate, several drugs have been reported to read through the specific stop codons of nonsense mutations, resulting in producing full-length proteins [9-11]. Therefore such "read-through" drugs might ameliorate severe congenital skin disorders if they are caused by the specific nonsense mutations. Since some subtypes of junctional EB have "hot spots" of nonsense mutations[12], there seems to be a space of novel gene-therapeutic agents in the future.

Congenital disorders that lack secretory proteins could be ameliorated by supplying the recombinant proteins systemically or locally. Several congenital metabolic disorders such as Fabry's disease have been already treated with enzyme replacement therapy[13]. Woodley and colleagues succeeded in the deposition of COL7 at the BMZ of artificially-constructed DEB skin by injecting recombinant COL7[14]. The same group later reported the amelioration of RDEB mice by injecting human COL7[15]. Other than secretory proteins like COL7, laminin beta-3, a structural protein in the BMZ, is found to be provided with protein therapy by protein transfection technique[16]. Protein therapies are safer than other novel therapies in the way that patients can attempt the therapy with lower dose of protein and that no gene correction is needed. Conversely, its effects are limited to the area of injection. The safety of the recombinant protein should be alarmed since bovine serum is generally essential for the culture of transfected cells. Efficient purification of large amount of protein is another challenge. The risk of immunoreactivity might weaken the effect of protein therapy and even cause exacerbation. In recessive DEB-generalized other type, the mutated COL7 protein partially function to form incomplete anchoring fibrils. Therefore, protein therapy-induced autoimmunity in such patients might inhibit the residual COL7 functions, resulting in exacerbation of blistering on the whole body.

Considering the clinical application of congenital disorders, the easiest source of normal proteins is allografts. Therefore, utilizing allogenic normal cells could be the fundamental therapeutic strategy. Applying allogenic keratinocytes, or allo-skin graft could treat congenital skin disorders, but allogenic keratinocytes are generally rejected because of their high immunogenicity. In order to overcome rejection, less immunogenic cells such as fibroblasts have been attempted to treat DEB. Intralesional injection of allogenic fibroblasts into DEB patients caused the deposition of COL7 for more than 3 months with matured anchoring fibrils[17]. Furthermore, intravenous injection of human fibroblasts into nude mice introduced human COL7 deposition in the BMZ of wound-healed skin[18]. Mesenchymal stem/stromal cells (MSCs) are another candidate for cell therapies; Conget and colleagues reported COL7 deposition at the site of intradermal injection of allogenic MSCs[19] in RDEB patient.

Another strategy of cell therapy is stem cell transplantation such as bone marrow transplantation (BMT) and cord-blood stem cell transplantation. If such stem cells engraft completely and provide functional stem cell-derived skin component cells from peripheral blood flow, systemic amelioration of EB will be accomplished for a long time without immunological rejection. Since stem cell transplantation has already performed widely for hematologic disorders and some congenital metabolic disorders, ethical and technical hurdles are much lower than gene/protein therapies.

Differentiation from bone marrow cells into functional keratinocytes

Stem cells in the bone marrow were recently found to have a pluripotency; a potential to differentiate into various cell lineages other than hematocytes. This pluripotency or transdifferentiation are observed more frequently in the injured organs such as damaged liver, ischemic heart, injured nerve tissues and wounded skin[20,21]. However, it had been unknown what causes efficient differentiation from bone marrow stem cells into injured skin, and whether these differentiated cells actually function like other normal organ cells.

Our group first revealed that a chemokine CTACK/CCL27 from the injured skin tissue accelerates the differentiation from bone marrow stem cells into epidermal keratinocytes[22]. Murine GFP-positive bone marrow cells were transplanted into normal mice, and the acceleration of wound healing and GFP-positive epidermal keratinocytes were investigated with or without local injection of CTACK/CCL27. Interestingly, CTACK/CCL27 enhanced the bone marrow-derived keratinocytes approximately 4 times, which was inhibited by anti-CTACK/CCL27 antibodies. Another chemokine SLC/CCL21 are similarly found to enhance wound healing via differentiating MSCs into various skin component cells including keratinocytes[23].

We also revealed that these differentiated keratinocytes actually function and provide BMZ component proteins. Focused on one basal keratinocyte-specific structural protein type XVII collagen (COL17), we prepared mice expressing normal murine Col17 (mCol17), transgenic mice expressing both murine and human COL17 (hCOL17) and COL17-humanized mice that express only hCOL17[24]. Interestingly, the expressions of donor bone marrow-derived COL17 in the skin were confirmed after performing BMTs among these mice of different COL17 expression patterns[25]. Since only keratinocytes express COL17 among skin-component cells and peripheral blood, bone marrow-derived keratinocytes are found to function and produce a BMZ component COL17.

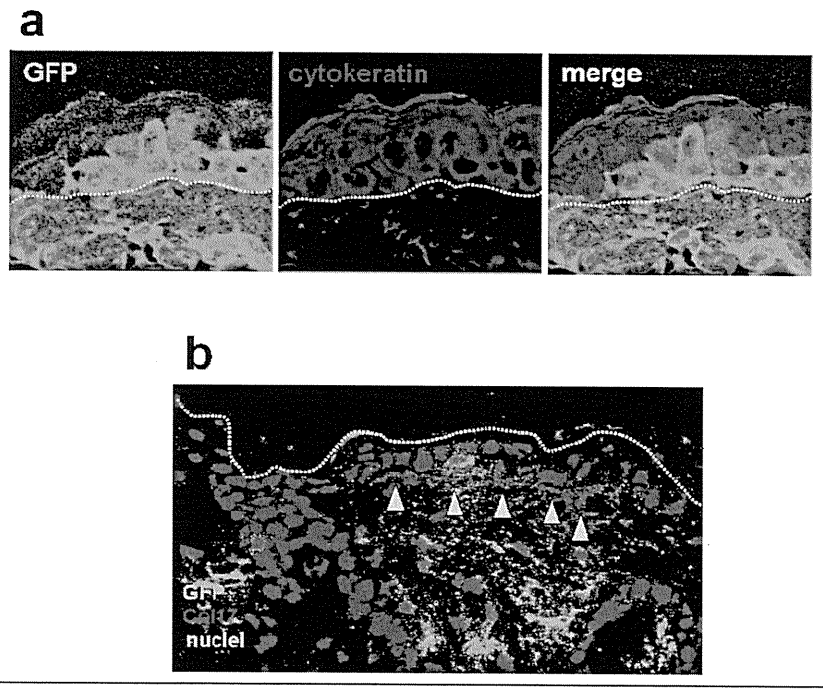

Fig. 2
Bone marrow transplantation into Col17 knockout JEB mice. (a) Donor-derived, GFP+ cytokeratin+ cells are aggregated in the basal cell layer of the epidermis, indicating bone marrow cells re-programmed into epidermal keratinocytes. (b) Immunofluorescence revealed GFP+ cells in the epidermis and dermis, with linear expression of Col17 in the BMZ.

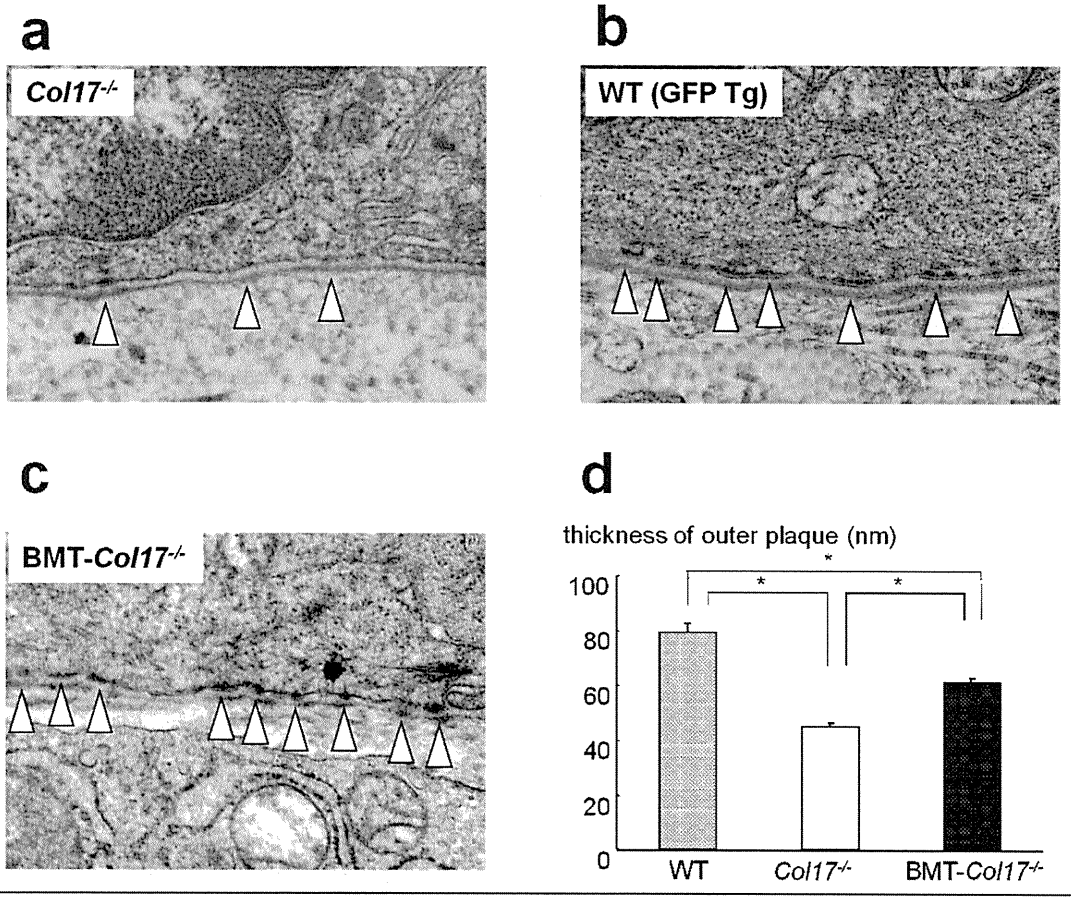

Fig. 3

Electron microscopy analysis in the skin after BMT into JEB mice. (a) Untreated Col17 knockout mice have thin, immature hemidesmosomes in the bottom of basal cell layer (arrowheads). (b) Normal C57BL/6 mice have mature, apparent hemidesmosomes. (c) Thick and matured hemidesmosomes are observed in the skin of BMT-treated Col17 knockout mice. (d) Thickness of the outer plaques of hemidesmosomes shows statistical improvement after BMT.

Stem cell therapy for epidermolysis bullosa

As mentioned previously, stem cell therapy is a promising strategy for systemic amelioration of EB for a long time. So far, a few investigations of BMT to treat RDEB have been published. Tolar *et al.* reported that hematopoietic stem cells contributed to life prolongation in RDEB model mice[26]. Chino *et al.* reported that treatment of embryonic BMT into RDEB model mice induced the expression of type VII collagen[27]. These reports proved the existence of donor-derived fibroblasts by immunohistochemistry and cell culture, and these fibroblasts are thought to produce type VII collagen. Based on these findings, hematopoietic stem cell therapies recently performed for RDEB patients in the US as a phase I/II clinical trial[28]. Five out of seven patients survived after the treatment, and less frequent dressings into the wound skin have achieved probably due to restoration of type VII collagen. These reports implied the benefit of stem cell transplantation in patients with deficient type VII collagen, which is produced by both epidermal keratinocytes and dermal fibroblasts[29]. Then, how is the clinical effect of stem cell transplantation in other subtype of EB, in which keratinocyte-specific skin component protein is lacked?

In order to answer the question we performed stem cell transplantation into adult Col17 knockout JEB model mice[25]. These treated mice expressed the lacked Col17 protein in the BMZ of the eroded skin around donor-derived GFP+ keratinocytes, with mature hemidesmosomes on the basal cells (Fig. 2, 3).

Clinical manifestations such as skin fragility and survival rates were also improved after stem cell transplantation (Fig. 4). Not only conventional BMT technique but hematopoietic stem cells transplantation and MSC infusion improved the expression of Col17. Furthermore, human hematopoietic stem cells also have a potential to restore epidermal component proteins by investigation of human-murine xeno-transplantation model, which implies stem cell transplantation might be a promising and fundamental therapeutic strategy for the treatment of severe EB patients.

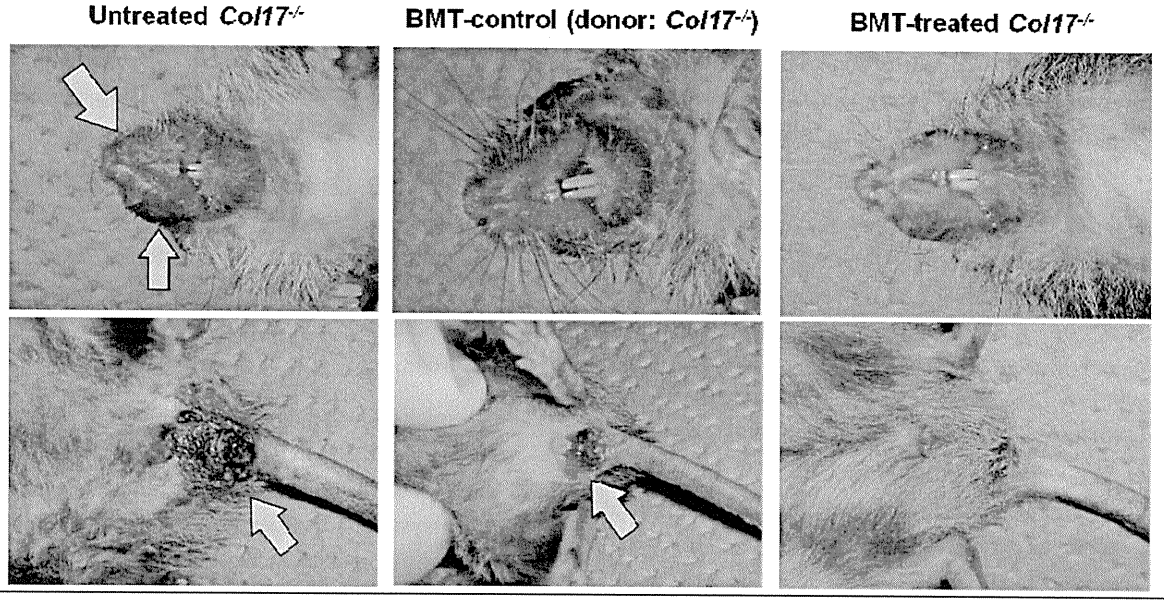

Fig. 4
Clinical manifestations of Col17 knockout mice after 120 days after birth (90 dayes after BMT). (left) Untreated Col17 knockout mice show erosions and ulcers on the perioral and perianal areas, which is compatible with clinical manifestations of JEB. (middle) As a control, BMT was performed from Col17 knockout mice into Col17 knockout mice. Severe erosions still appear as untreated mice. (right) Therapeutic BMT from GFP+ mice caused less severe erosions.

There still have problems to overcome on the stem cell transplantation for severe EB patients; *e.g.* risk of infection, conditioning regimens and donor supply. Although stem cell transplantation is prevalent, treatment-related deaths do occur due to severe infection, regimen-related toxicity and graft-versus-host disease (GVHD). Since EB patients have sevère erosion and blisters on the whole body, severe cutaneous infections during the treatment could be fatal[28,30]. Conditioning regimens and the consideration of mini-transplantation should be determined carefully to avoid severe GVHD; both GVHD and regimen-related toxicity could cause severe erosions that are indistinguishable from EB symptoms. The donor is another challenge. Related HLA-matched siblings without EB phenotype are ideal for donors, but few cases meet the condition[28]. Unrelated HLA-matched stem cells from donor coordination programs, T-cell depleted haploidentical stem cell transplantation and iPS cell-bank projects might open the door to stem cell therapies in the future[31,32].

Concluding remarks

Stem cell therapies have been emerged as a promising strategy for congenital severe skin disorders such as EB. Although merits and demerits should be considered compared to gene therapies and protein therapies, novel treatments from the view of regenerative medicine will be one of the main streams to provide fundamental answers for severe disorders.

References

1) Shimizu H: Structure and Function of the Skin. Shimizu's Textbook of Dermatology, Nakayama Shoten Co., Ltd., Tokyo. 2007; 6.

2) Fine JD, Eady RA, Bauer EA, Bauer JW, Bruckner-Tuderman L, Heagerty A, Hintner H, Hovnanian A, Jonkman MF, Leigh I, McGrath JA, Mellerio JE, Murrell DF, Shimizu H, Uitto J, Vahlquist A,

Woodley D, Zambruno G: The classification of inherited epidermolysis bullosa (EB): Report of the Third International Consensus Meeting on Diagnosis and Classification of EB. J Am Acad Dermatol. 2008; 58: 931-950.

3) Mavilio F, Pellegrini G, Ferrari S, Di Nunzio F, Di Iorio E, Recchia A, Maruggi G, Ferrari G, Provasi E, Bonini C, Capurro S, Conti A, Magnoni C, Giannetti A, De Luca M: Correction of junctional epidermolysis bullosa by transplantation of genetically modified epidermal stem cells. Nat Med. 2006; 12: 1397-1402.

4) Gabriel R, Eckenberg R, Paruzynski A, Bartholomae CC, Nowrouzi A, Arens A, Howe SJ, Recchia A, Cattoglio C, Wang W, Faber K, Schwarzwaelder K, Kirsten R, Deichmann A, Ball CR, Balaggan KS, Yanez-Munoz RJ, Ali RR, Gaspar HB, Biasco L, Aiuti A, Cesana D, Montini E, Naldini L, Cohen-Haguenauer O, Mavilio F, Thrasher AJ, Glimm H, von Kalle C, Saurin W, Schmidt M: Comprehensive genomic access to vector integration in clinical gene therapy. Nat Med. 2009; 15: 1431-1436.

5) Takahashi K, Yamanaka S: Induction of pluripotent stem cells from mouse embryonic and adult fibroblast cultures by defined factors. Cell. 2006; 126: 663-676.

6) Hanna J, Wernig M, Markoulaki S, Sun CW, Meissner A, Cassady JP, Beard C, Brambrink T, Wu LC, Townes TM, Jaenisch R: Treatment of sickle cell anemia mouse model with iPS cells generated from autologous skin. Science. 2007; 318: 1920-1923.

7) Tolar J, Xia L, Riddle MJ, Lees CJ, Eide CR, McElmurry RT, Titeux M, Osborn MJ, Lund TC, Hovnanian A, Wagner JE, Blazar BR: Induced pluripotent stem cells from individuals with recessive dystrophic epidermolysis bullosa. J Invest Dermatol. 2011; 131: 848-856.

8) De Luca M, Pellegrini G, Mavilio F: Gene therapy of inherited skin adhesion disorders: a critical overview. Br J Dermatol. 2009; 161: 19-24.

9) Kerem E, Hirawat S, Armoni S, Yaakov Y, Shoseyov D, Cohen M, Nissim-Rafinia M, Blau H, Rivlin J, Aviram M, Elfring GL, Northcutt VJ, Miller LL, Kerem B, Wilschanski M: Effectiveness of PTC124 treatment of cystic fibrosis caused by nonsense mutations: a prospective phase II trial. Lancet. 2008; 372: 719-727.

10) Lai CH, Chun HH, Nahas SA, Mitui M, Gamo KM, Du L, Gatti RA: Correction of ATM gene function by aminoglycoside-induced read-through of premature termination codons. Proc Natl Acad Sci U S A. 2004; 101: 15676-15681.

11) Wilschanski M, Yahav Y, Yaacov Y, Blau H, Bentur L, Rivlin J, Aviram M, Bdolah-Abram T, Bebok Z, Shushi L, Kerem B, Kerem E: Gentamicin-induced correction of CFTR function in patients with cystic fibrosis and CFTR stop mutations. N Engl J Med. 2003; 349: 1433-1441.

12) Posteraro P, De Luca N, Meneguzzi G, El Hachem M, Angelo C, Gobello T, Tadini G, Zambruno G, Castiglia D: Laminin-5 mutational analysis in an Italian cohort of patients with junctional epidermolysis bullosa. J Invest Dermatol. 2004; 123: 639-648.

13) Desnick RJ, Brady R, Barranger J, Collins AJ, Germain DP, Goldman M, Grabowski G, Packman S, Wilcox WR: Fabry disease, an under-recognized multisystemic disorder: expert recommendations for diagnosis, management, and enzyme replacement therapy. Ann Intern Med. 2003; 138: 338-346.

14) Woodley DT, Keene DR, Atha T, Huang Y, Lipman K, Li W, Chen M: Injection of recombinant human type VII collagen restores collagen function in dystrophic epidermolysis bullosa. Nat Med. 2004; 10: 693-695.

15) Remington J, Wang X, Hou Y, Zhou H, Burnett J, Muirhead T, Uitto J, Keene DR, Woodley DT, Chen M: Injection of recombinant human type VII collagen corrects the disease phenotype in a murine model of dystrophic epidermolysis bullosa. Mol Ther. 2009; 17: 26-33.

16) Igoucheva O, Kelly A, Uitto J, Alexeev V: Protein therapeutics for junctional epidermolysis bullosa: incorporation of recombinant beta3 chain into laminin 332 in beta3-/- keratinocytes in vitro. J Invest Dermatol. 2008; 128: 1476-1486.

17) Wong T, Gammon L, Liu L, Mellerio JE, Dopping-Hepenstal PJ, Pacy J, Elia G, Jeffery R, Leigh IM, Navsaria H, McGrath JA: Potential of fibroblast cell therapy for recessive dystrophic epidermolysis bullosa. J Invest Dermatol. 2008; 128: 2179-2189.

18) Woodley DT, Remington J, Huang Y, Hou Y, Li W, Keene DR, Chen M: Intravenously injected human fibroblasts home to skin wounds, deliver type VII

collagen, and promote wound healing. Mol Ther. 2007; 15: 628-635.

19) Conget P, Rodriguez F, Kramer S, Allers C, Simon V, Palisson F, Gonzalez S, Yubero MJ: Replenishment of type VII collagen and re-epithelialization of chronically ulcerated skin after intradermal administration of allogeneic mesenchymal stromal cells in two patients with recessive dystrophic epidermolysis bullosa. Cytotherapy. 2010; 12: 429-431.

20) Ferrari G, Cusella-De Angelis G, Coletta M, Paolucci E, Stornaiuolo A, Cossu G, Mavilio F: Muscle regeneration by bone marrow-derived myogenic progenitors. Science. 1998; 279: 1528-1530.

21) Lagasse E, Connors H, Al-Dhalimy M, Reitsma M, Dohse M, Osborne L, Wang X, Finegold M, Weissman IL, Grompe M: Purified hematopoietic stem cells can differentiate into hepatocytes in vivo. Nat Med. 2000; 6: 1229-1234.

22) Inokuma D, Abe R, Fujita Y, Sasaki M, Shibaki A, Nakamura H, McMillan JR, Shimizu T, Shimizu H: CTACK/CCL27 accelerates skin regeneration via accumulation of bone marrow-derived keratinocytes. Stem cells (Dayton, Ohio). 2006; 24: 2810-2816.

23) Sasaki M, Abe R, Fujita Y, Ando S, Inokuma D, Shimizu H: Mesenchymal stem cells are recruited into wounded skin and contribute to wound repair by transdifferentiation into multiple skin cell type. J Immunol. 2008; 180: 2581-2587.

24) Nishie W, Sawamura D, Goto M, Ito K, Shibaki A, McMillan JR, Sakai K, Nakamura H, Olasz E, Yancey KB, Akiyama M, Shimizu H: Humanization of autoantigen. Nat Med. 2007; 13: 378-383.

25) Fujita Y, Abe R, Inokuma D, Sasaki M, Hoshina D, Natsuga K, Nishie W, McMillan JR, Nakamura H, Shimizu T, Akiyama M, Sawamura D, Shimizu H: Bone marrow transplantation restores epidermal basement membrane protein expression and rescues epidermolysis bullosa model mice. Proc Natl Acad Sci U S A. 2010; 107: 14345-14350.

26) Tolar J, Ishida-Yamamoto A, Riddle M, McElmurry RT, Osborn M, Xia L, Lund T, Slattery C, Uitto J, Christiano AM, Wagner JE, Blazar BR: Amelioration of epidermolysis bullosa by transfer of wild-type bone marrow cells. Blood. 2009; 113: 1167-1174.

27) Chino T, Tamai K, Yamazaki T, Otsuru S, Kikuchi Y, Nimura K, Endo M, Nagai M, Uitto J, Kitajima Y, Kaneda Y: Bone marrow cell transfer into fetal circulation can ameliorate genetic skin diseases by providing fibroblasts to the skin and inducing immune tolerance. Am J Pathol. 2008; 173: 803-814.

28) Wagner JE, Ishida-Yamamoto A, McGrath JA, Hordinsky M, Keene DR, Woodley DT, Chen M, Riddle MJ, Osborn MJ, Lund T, Dolan M, Blazar BR, Tolar J: Bone marrow transplantation for recessive dystrophic epidermolysis bullosa. N Engl J Med. 2010; 363: 629-639.

29) Goto M, Sawamura D, Ito K, Abe M, Nishie W, Sakai K, Shibaki A, Akiyama M, Shimizu H: Fibroblasts show more potential as target cells than keratinocytes in COL7A1 gene therapy of dystrophic epidermolysis bullosa. J Invest Dermatol. 2006; 126: 766-772.

30) Kopp J, Horch RE, Stachel KD, Holter W, Kandler MA, Hertzberg H, Rascher W, Campean V, Carbon R, Schneider H: Hematopoietic stem cell transplantation and subsequent 80% skin exchange by grafts from the same donor in a patient with Herlitz disease. Transplantation. 2005; 79: 255-256.

31) Sodani P, Isgro A, Gaziev J, Polchi P, Paciaroni K, Marziali M, Simone MD, Roveda A, Montuoro A, Alfieri C, De Angelis G, Gallucci C, Erer B, Isacchi G, Zinno F, Adorno G, Lanti A, Faulkner L, Testi M, Andreani M, Lucarelli G: Purified T-depleted, CD34+ peripheral blood and bone marrow cell transplantation from haploidentical mother to child with thalassemia. Blood. 2010; 115: 1296-1302.

32) Stern M, Ruggeri L, Mancusi A, Bernardo ME, de Angelis C, Bucher C, Locatelli F, Aversa F, Velardi A: Survival after T cell-depleted haploidentical stem cell transplantation is improved using the mother as donor. Blood. 2008; 112: 2990-2995.

Australasian Journal of Dermatology

Australasian Journal of Dermatology (2011) 52, e1–e4 doi: 10.1111/j.1440-0960.2010.00684.x

CASE REPORT

Autosomal dominant bullous dermolysis of the newborn associated with a heterozygous missense mutation p.G1673R in type VII collagen

John Frew,[1] Shueh W Lim,[3] Alfred Klausseger,[5] Chung W Chow,[4] Kim Tran,[2] John Su,[4] David Orchard,[4] George Varigos,[4] Daisuke Sawamura,[6] Wataru Nishie,[6] Hiroshi Shimizu[6] and Dédée F Murrell[1]

Departments of [1]Dermatology and [2]Anatomical Pathology, St George Hospital, University of New South Wales, Sydney, New South Wales, [3]Department of Dermatology, Austin Hospital, [4]Department of Dermatology, Royal Children's Hospital, Melbourne, Victoria, Australia; [5]EB-Haus, Salzburg, Austria; and [6]Department of Dermatology, Hokkaido University Graduate School of Medicine, Sapporo, Japan

ABSTRACT

Bullous dermolysis of the newborn is an inherited mechano-bullous disorder classed as a rare subtype of dystrophic epidermolysis bullosa. Fewer than 30 cases of bullous dermolysis of the newborn have been reported in the literature and the pathogenesis of the disease is poorly understood. Only a minority of cases have had pathogenic mutations identified. We present a case of a neonate born to non-consanguineous Caucasian parents with an exon 54 (c.5017G > A, p.G1673R) mutation reported as one mutant allele in a case of recessive dystrophic epidermolysis bullosa (generalized other).

Key words: bullous dermolysis of the newborn, genodermatoses, type VII collagen.

INTRODUCTION

Bullous dermolysis of the newborn (BDN) is an inherited mechano-bullous disorder classed as a rare subtype of dystrophic epidermolysis bullosa (DEB) and classified according to its inheritance as an autosomal dominant DEB-BDN or recessive DEB-BDN disorder.[1,2] It is characterized by blistering of the skin at birth in the setting of mechanical trauma, with subsequent improvement or complete resolution of symptoms over the ensuing months of life (OMIM 131705). Initial neonatal blistering can be widespread, involving the trunk and extremities. It occasionally affects the nails and mucous membranes and typically resolves by the end of the first year of life. Healing typically occurs without scarring, although permanent scarring has been reported.[2,3]

Fewer than 30 cases of BDN have been reported in the literature since the identification of the disease in 1985.[4] The pathogenesis of the disease is poorly understood; however, mutations in the collagen VII gene (*COL7A1*) have been implicated. Only a minority of cases have had pathogenic mutations identified.[2–8] The poor understanding of the disease process has detrimental implications in the accurate prognostication of neonatal blistering disorders.

We present a recent case of BDN involving a novel pathogenic *COL7A1* mutation. This mutation has also been described[6] in what was previously known as non-Hallopeau–Siemens recessive RDEB, now known as generalized other RDEB (RDEB-O).[1]

Main text

A male infant (Australasian EB Registry Patient Number: 234)[9] was born at 37 weeks gestation in November 2006 after an uncomplicated pregnancy to a mother of gravida 2, parity 0. The mother's first pregnancy underwent a

Correspondence: Professor Dédée Murrell, Department of Dermatology, Ground Floor, James Laws House, St George Hospital, Gray St, Kogarah, NSW 2217, Australia. Email: d.murrell@unsw.edu.au

John Frew, MB BS. Shueh W Lim, FACD. Alfred Klausseger, MSc. Chung W Chow, FRCPA. Kim Tran, FRCPA. John Su, FACD. David Orchard, FACD. George Varigos, FACD. Daisuke Sawamura, PhD. Wataru Nishie, PhD. Hiroshi Shimizu, PhD. Dédée F Murrell, FAAD.

Submitted 6 April 2010; accepted 6 June 2010.

Abbreviations:

BDN	bullous dermolysis of the newborn
DEB	dystrophic epidermolysis bullosa
RDEB-O	generalized other recessive DEB

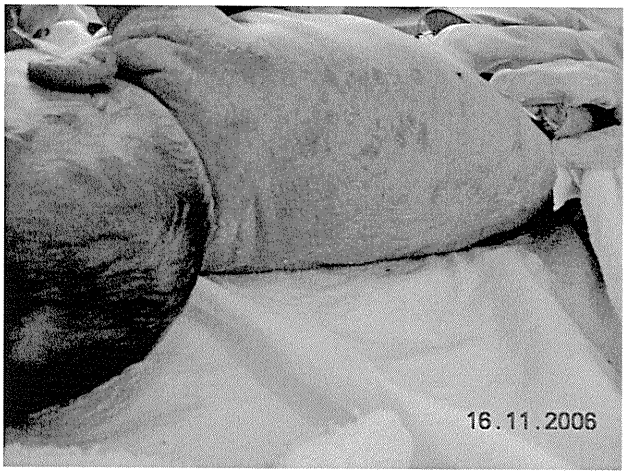

Figure 1 Neonate demonstrating blisters at birth.

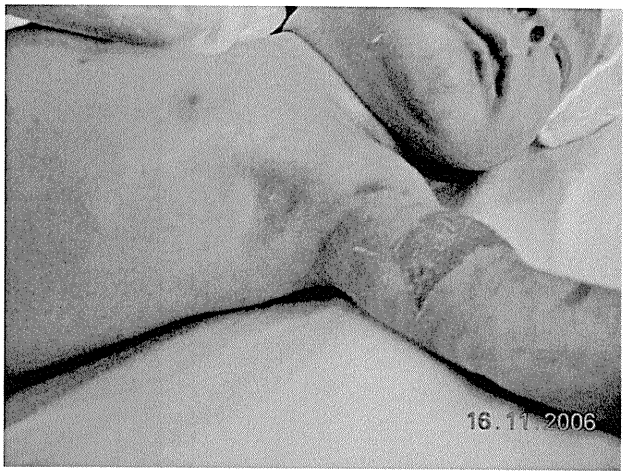

Figure 2 Blister caused by adhesive tape.

termination for reasons unrelated to the present case. The parents were non-consanguineous Caucasian Australians of British descent and had no previous children. The neonate was born with multiple erosions and erythematous patches that subsequently developed into confluent bullae on the trunk and extremities over the following hours (Fig. 1). The infant displayed neither mucosal involvement nor dysmorphic features and was otherwise systemically well.

Initial investigations of the proband included swabs of the eroded areas for microscopy, culture and sensitivity, Blood cultures were taken and intravenous flucloxacillin and gentamicin were initiated. On the second day of life, bullae were evident on the site where the cannula was secured to the arm with adhesive tape, and on other sites of mild mechanical trauma (Fig. 2). Subsequently, skin biopsies, light microscopy, immunofluorescence mapping (Fig. 3) and electron microscopy (Fig. 3) were undertaken.

Over the next 2 months, the severity and number of blisters and erosions decreased and previous blisters resolved without scarring. At 18 months of age, blistering had ceased and the only manifestations seen were milia on the palmar surface of the hands.

Differential diagnoses included Staph scalded skin syndrome, impetigo, toxic epidermal necrosis and epidermolysis bullosa.

Investigative results

Skin biopsies of the blisters showed sub-basal dermoepidermal separation below the level of the lamina densa. Immunofluorescence mapping showed reduced intensity staining with the LH7.2 antibody to collagen VII and basal as well as suprabasal collections of collagen VII (Fig. 3). Electron microscopy demonstrated a paucity of dermal anchoring fibrils and highly dilated endoplasmic reticula, forming stellate bodies within basal keratinocytes (Fig. 3).

The infant's genomic DNA from blood was found to be heterozygous for a missense mutation (Fig. 3) on exon 54 of *COL7A1* (c.5017G > A, p.G1673R) not previously described in BDN.[6,10] A second sequence variant on exon 5 was identified (c.592G > A, p.V198I); however, this was considered unlikely to be pathogenic. Both of these mutations were paternal in origin. In order to clarify the nature of the second sequence variant a polymorphism study was undertaken, screening 145 wildtype samples from a normal Caucasian European population for the c.592G > A, p. V198I sequence variant using polymerase chain reaction and direct sequencing. It was found in one of the 145 samples.

DISCUSSION

Bullous dermolysis of the newborn is characterized histologically by blister formation at the dermoepidermal junction, just below the level of the lamina densa. Dermal anchoring fibrils are reduced in number and quality, while epidermal collections of collagen VII are evident.[2] Electron microscopy reveals grossly dilated endoplasmic reticula of basal and suprabasal keratinocytes, known as 'stellate bodies'. The pathogenesis of BDN involves a defect in the intracytoplasmic packaging or transport of collagen VII in basal keratinocytes;[2] however, the underlying explanation of why specific mutations in *COL7A1* result in a transient as opposed to a permanent deficiency of anchoring fibrils is unclear. Only four *COL7A1* mutations have been previously described in BDN and none of the aforementioned mutations have been described in cases of recessive or dominant DEB.[10]

Previously described mutations in BDN include an acceptor splice site mutation in intron 35 of COL7A1 (4120-1G > C)8 and two cases involving glycine substitution mutations; p.G1522E[2] and a heterozygote for p.G1519D/p.G2251E.[5] In the latter case, p.G2251E was presumed to be the pathogenic mutation, as carriers for this polymorphism also displayed mild DEB characteristics such as nail dystro-

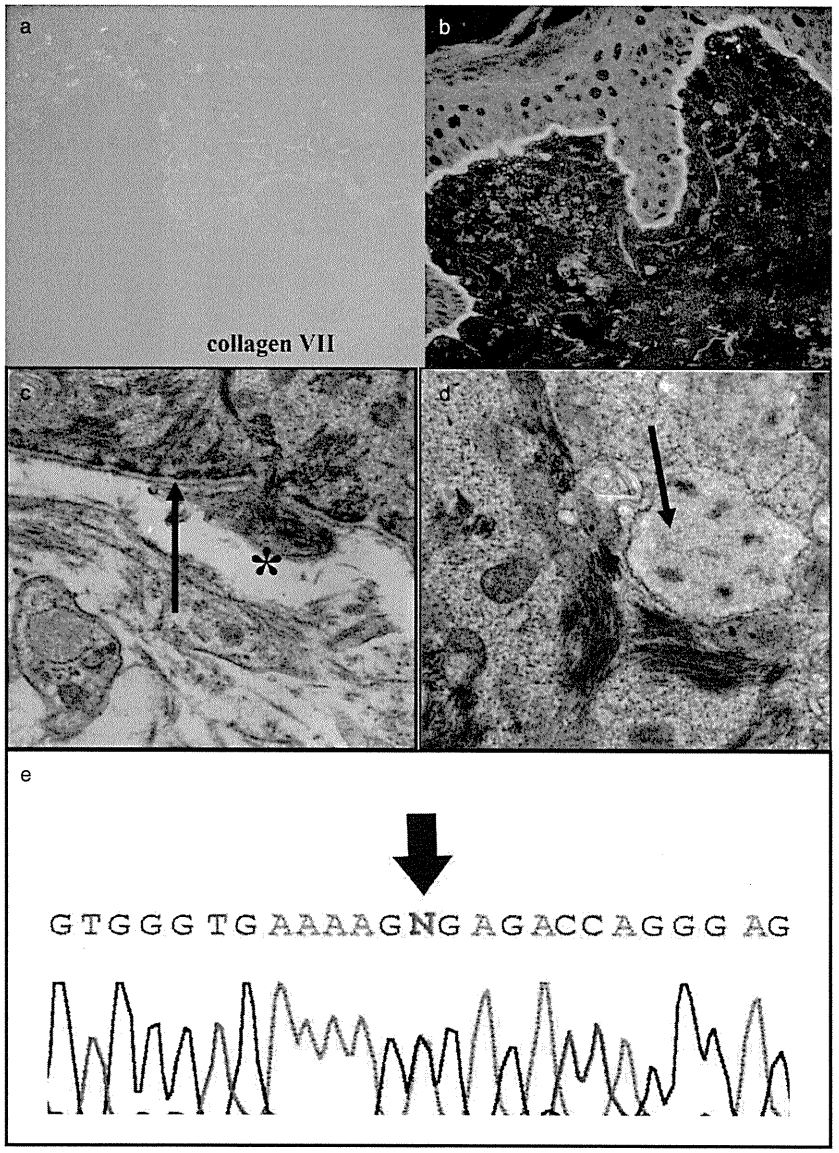

Figure 3 (a) Immunofluorescence mapping: stippled staining in the epidermis and lack of linear staining at the dermoepidermal junction, consistent with bullous dermolysis of the newborn (×20). (b) Control sample. (c) Electron microscopy showing the plane of cleavage (*) the basal lamina (arrow) and (d) typical keratinocyte 'stellate bodies' (arrow) (×10 000). (e) Genomic sequence data showing the missense mutation in exon 54 of *COL7A1*.

phy. The missense mutation in exon 54 (c.5017G > A, p.G1673R) has been previously described in another Caucasian family with RDEB-O;[6] however, the second mutation was not identified. Direct sequencing of exon 54 in 70 unrelated wildtype samples failed to identify the mutation (c.5017G > A, p.G1673R), indicating that it is not a neutral polymorphism. However, it may be possible that this glycine substitution is both a dominant and recessive mutation.

With regards to the exon 5 sequence variant, our polymorphism studies detected this genetic variation (V198I) once in 145 wildtype samples taken from a Caucasian European population. This suggests that the sequence variant is a rare single nucleotide polymorphism that is unlikely to be pathogenic. We postulate that this polymorphism is likely to lie on the same paternal allele of COL7A1, as the father and son both have the two mutations. Unfortunately, the mother declined genetic testing.

CONCLUSION

In summary, we present a case of autosomal dominant BDN in whom a linked *COL7A1* sequence variant has been identified which has been previously described in RDEB-O. Although the mechanism and pathogenesis of BDN is poorly understood, the fact that this mutation is also present in a previously described case of RDEB-O gives scope for hypotheses into how these two different diseases with different prognoses can coexist whilst sharing a pathogenic mutation. An increased understanding of the genotype–phenotype correlations in BDN may lead to a deeper

understanding of the mechanisms underlying defects in collagen VII production and transportation, which may in the future lead to therapeutic advancements for these disabling and disfiguring diseases.

REFERENCES

1. Fine J-D, Eady RA, Bauer E *et al.* The classification of inherited epidermolysis bullosa (EB): Report of the Third International Consensus Meeting on Diagnosis and Classification of EB. *J. Am. Acad. Dermatol.* 2008; **58**: 931–50.
2. Fassihi H, Diba VC, Wessagowit V *et al.* Transient bullous dermolysis of the newborn in three generations. *Br. J. Dermatol.* 2005; **153**: 1058–63.
3. Hanson S, Fine J-D, Levy ML. Three new cases of transient bullous dermolysis of the newborn. *J. Am. Acad. Derm.* 1999; **40**: 471–6.
4. Hashimoto K, Matsumoto H, Iacobelli D. Transient bullous dermolysis of the newborn. *Arch. Derm.* 1985; **121**: 1429–38.
5. Hammami-Hauasli N, Raghunath M, Kuster W *et al.* Transient bullous dermolysis of the newborn associated with compound heterozygosity for recessive and dominant COL7A1 mutations. *J. Invest. Dermatol.* 1998; **111**: 1214–19.
6. Dang N, Murrell DF. Mutation analysis and characterization of COL7A1 mutations in dystrophic epidermolysis bullosa. *Exp. Dermatol.* 2008; **17**: 553–68.
7. Nakano H, Toyomaki Y, Ohashi S *et al.* Novel COL7A1 mutations in a Japanese family with transient bullous dermolysis of the newborn associated with pseudosyndactyly. *Br. J. Dermatol.* 2007;**157**: 179–82.
8. Christiano AM, Fine J-D UJ. Genetic basis of dominantly inherited transient bullous dermolysis of the newborn: a splice site mutation in the type VII collagen gene. *J. Invest. Dermatol.* 1997; **109**: 811–14.
9. Kho YC, Agero AL, Rhodes LM *et al.* Epidemiology of EB in the antipodes: the Australasian EB registry with a focus on Herlitz junctional EB. *Arch. Dermatol.* 2010; **146**: 635–40.
10. Varki R, Sadowski S, Uitto J *et al.* Epidermolysis bullosa II. Type VII collagen mutations and phenotype-genotype correlations in the dystrophic subtypes. *J. Med. Genet.* 2007; **44**: 181–92.

available at www.sciencedirect.com

ScienceDirect

journal homepage: www.elsevier.com/locate/burns

Second harmonic generation and multiphoton microscopic detection of collagen without the need for species specific antibodies

Alice C.-H. Chen [a], *Celia McNeilly* [b], *Ashley P.-Y. Liu* [a], *Christopher J. Flaim* [b], *Leila Cuttle* [a], *Mark Kendall* [b], *Roy M. Kimble* [a], *Hiroshi Shimizu* [c], *James R. McMillan* [a,*]

[a] *The Centre for Children's Burns Research, Queensland Children's Medical Research Institute, Royal Children's Hospital, The University of Queensland, Brisbane, QLD 4029, Australia*

[b] *Australian Institute for Bioengineering and Nanotechnology, The University of Queensland, Brisbane, QLD 4072, Australia*

[c] *Department of Dermatology, Hokkaido University Graduate School of Medicine, Sapporo, Japan*

ARTICLE INFO

Article history:
Accepted 21 March 2011

Keywords:
Multi-photon microscope
Second harmonic generation
Collagen
Burn wound
Scar

ABSTRACT

High-resolution, high-contrast, three-dimensional images of live cell and tissue architecture can be obtained using second harmonic generation (SHG), which comprises non-absorptive frequency changes in an excitation laser line. SHG does not require any exogenous antibody or fluorophore labeling, and can generate images from unstained sections of several key endogenous biomolecules, in a wide variety of species and from different types of processed tissue. Here, we examined normal control human skin sections and human burn scar tissues using SHG on a multi-photon microscope (MPM). Examination and comparison of normal human skin and burn scar tissue demonstrated a clear arrangement of fibers in the dermis, similar to dermal collagen fiber signals. Fluorescence-staining confirmed the MPM-SHG collagen colocalization with antibody staining for dermal collagen type-I but not fibronectin or elastin. Furthermore, we were able to detect collagen MPM-SHG signal in human frozen sections as well as in unstained paraffin embedded tissue sections that were then compared with hematoxylin and eosin staining in the identical sections. This same approach was also successful in localizing collagen in porcine and ovine skin samples, and may be particularly important when species-specific antibodies may not be available. Collectively, our results demonstrate that MPM SHG-detection is a useful tool for high resolution examination of collagen architecture in both normal and wounded human, porcine and ovine dermal tissue.

1. Introduction

Multi-photon microscopy (MPM) is a nonlinear optical phenomenon that provides intrinsic optical sectioning of a specimen, and can provide high-resolution, high-contrast three-dimensional views of live cell and tissue architecture. Several extracellular matrix (ECM) components and key endogenous biomolecules can be visualized *in situ* without the need for tissue processing and staining, exogenous

* *Corresponding author at*: The University of Queensland, The Centre for Children's Burns Research, Queensland Children's Medical Research Institute, Level 4 Foundation Building, Royal Children's Hospital, Brisbane, QLD 4029, Australia. Tel.: +61 7 3636 9069; fax: +61 7 3365 5455.
E-mail address: j.mcmillan@uq.edu.au (J.R. McMillan).

0305-4179/$36.00.
doi:10.1016/j.burns.2011.03.013

antibody labeling or fluorophores. These include the autofluorescence from reducing coenzyme NAD(P)H, flavoproteins, keratin, melanin, and elastin [1]. In addition, detection of second-harmonic generation (SHG), the non-absorptive frequency changes in an excitation laser line can also be performed using MPM. SHG is a nonlinear optical effect that results in an emission wavelength that is half the excitation wavelength. Myosin, tubulin and collagen polymeric proteins have previously been studied using SHG [2–4]. Recent studies have used SHG signals to look at various skin disorders [1,5], and even immune cell migration in the skin [6]. Furthermore, it has also been shown to be a powerful tool in tissue engineering and can be used to monitor drug delivery [7,8].

In human skin, collagen makes up 70% of the dry weight of the dermis. Dermal fibroblasts are responsible for regulating the steady state synthesis of collagen deposition in normal skin. Several matrix metalloproteinases (MMPs 1, 2, 3, 8, 9, 13, 18) are responsible for collagen degradation, hence maintaining collagen-tissue equilibrium [9]. The balance between collagen production by (myo-)fibroblasts and collagen degradation by matrix metalloproteinases determines the precise collagen bundle size and hence dermal thickness during the process of post wounding dermal remodeling. After massive burn injury, granulation tissue formation and dermal remodeling takes place to fill and repair the damaged tissue. With deep dermal burns, this often results in an unsightly, raised hypertrophic scar. The scars are usually active for more than six months after injury, and mature after 18 months [10,11]. However, the orientation and distribution of collagen fiber arrangement at different time points after burn and in the pathophysiology of hypertrophic scar formation is still unclear.

It is well understood that hypertrophic scars have different collagen organization compared to normal skin, and that collections of parallel fibers and collagen nodules can be observed at different stages of scarring [12]. Several studies have been carried out to observe collagen architecture in hypertrophic scars, however many of the methods for detecting the presence of dermal collagens have been costly, time consuming and involved immunohistochemical antibody staining on tissue sections. In addition, studies using animal models often face difficulties finding species-specific antibodies, and there is also a need for *in vivo* imaging techniques to be developed. This study attempted to use an alternative higher-resolution microscopic method to assess collagen fiber arrangements in control and burn scar skin tissues. We examined human, porcine and ovine normal skin sections and compared these to dermal tissue at several different stages after burn using MPM based on SHG, and determined that MPM detection of SHG is a powerful tool for examination of collagen architecture in skin.

2. Materials and methods

2.1. *Sample preparation*

This research has been approved by the Royal Children's Hospital and Health Services District Human Research Ethics Committee and all studies were performed in accordance with the Helsinki declaration. Normal Human and scar tissue sections were collected from scar excision surgeries in the Royal Children's Hospital in Brisbane, Australia. Two surgically removed human foreskin tissues were also collected to represent normal human tissues (Table 1). Both donors were less than 12 months of age. The scar tissue donors were Asian girls aged 10 and 11 with burn scar tissue collected from the upper aspect of the foot and right thigh respectively approximately three years after the initial burn. All skin tissues collected were (1) fixed in 4% formalin, embedded in paraffin, and (2) embedded in OCT (embedding medium for frozen tissue to ensure Optimal Cutting Temperature) and snap frozen in liquid nitrogen, with sections cut at 5 microns (μm). Porcine normal and scar skin sections used in this experiment were first described by Cuttle et al. [13]. Burns were created on Large White juvenile pigs of approximately 8 weeks of age using 92 °C water for 15 s. A deep dermal partial thickness burn was created, with hypertrophic scarring observed after 99 days. Hypertrophic scar and normal skin samples were collected and fixed in 4% formalin, then embedded in paraffin. Skin samples of two pigs were used in this study. Ovine skin sections used in this experiment were first described by Fraser et al. [14]. Burns were created on Merino ewe fetuses at 80 days gestation using 66 °C water for 7 s and the tissue collected at 60 days post-burn. Merino ewe lambs were burned with 82 °C water for 10 s at 28–30 days of age and the tissue was collected 1 day later. Burn and normal skin samples were collected at several time points and fixed in 10% formalin then embedded in paraffin. Skin samples of three ovine fetuses and two ovine lambs were used in this study. All samples were examined in duplicate.

Table 1 – The origin, age and location of tissues used in this study.

Sample	Species	Age	Time after burn	Gender	Body site	Ethnic background/ species type
Normal 1	Human	Less than 1 year	–	Male	Foreskin	Caucasian
Normal 2	Human	Less than 1 year	–	Male	Foreskin	Caucasian
Scar 1	Human	10 years	40 months	Female	Ankle	Asian
Scar 2	Human	11 years	44 months	Female	Right thigh	Asian
Porcine normal/porcine scar	Porcine	22 weeks	99 days	Female	Right flank	Large White pig
Fetus normal/fetus burn	Ovine	140 days fetal gestation (term = 145–150 days)	60 days	–	Flank	Merino ewes
Lamb normal/lamb burn	Ovine	4 weeks	1 day	Male	Lower abdomen	Merino ewes

2.2. *Multiphoton microscopy*

A Zeiss 510 Meta NLO multi-photon microscope (Zeiss, North Ryde, NSW, Australia) was used to detect the SHG signal from both frozen sections and paraffin sections to determine the optimal spectral parameters for SHG excitation and signal collection for each technique (frozen or paraffin), species (human or pig) and specimen (normal skin or burn scar) types. Previous studies have used an excitation wavelength of 800–860 nm to detect collagen SHG [15–18], therefore here we used the BP 390–465 filter (collection wavelength of 390–465 nm) to cover the excitation wavelengths from 780 to 930 nm. Systematic checking of each excitation wavelength for optimal collagen visualization was performed by preliminary excitation wavelength screening at 10 nm intervals ranging from 790 nm to 920 nm. The 20× objective lens was used throughout this experiment (SHG and H&E visualizations). In order to confirm that the SHG signal detected was in fact specific for collagen, sequential SHG and Alexa488 fluorescent signals from immunohistochemically stained tissue sections were collected. Colocalization of SHG signal and Alexa488 was performed using the optimally determined SHG excitation/emission wavelength combination together with a second channel collecting the 500–550 nm emission from Alexa 488 (excited by a 488 nm laser). Zeiss AIM software was used to visualize the images. After SHG imaging both cryostat and paraffin sections were stained using routine hematoxylin and eosin (H&E) staining methods with acetone pre-treatment for cryostat sections [19].

2.3. *Indirect immunofluorescent staining*

For collagen I and fibronectin staining on frozen sections, slides were incubated in 10% goat serum (Millipore, CA, USA) blocking solution for 30 min, then incubated in a 1:100 dilution of collagen I monoclonal antibody ([COL-1] ab6308 Abcam,

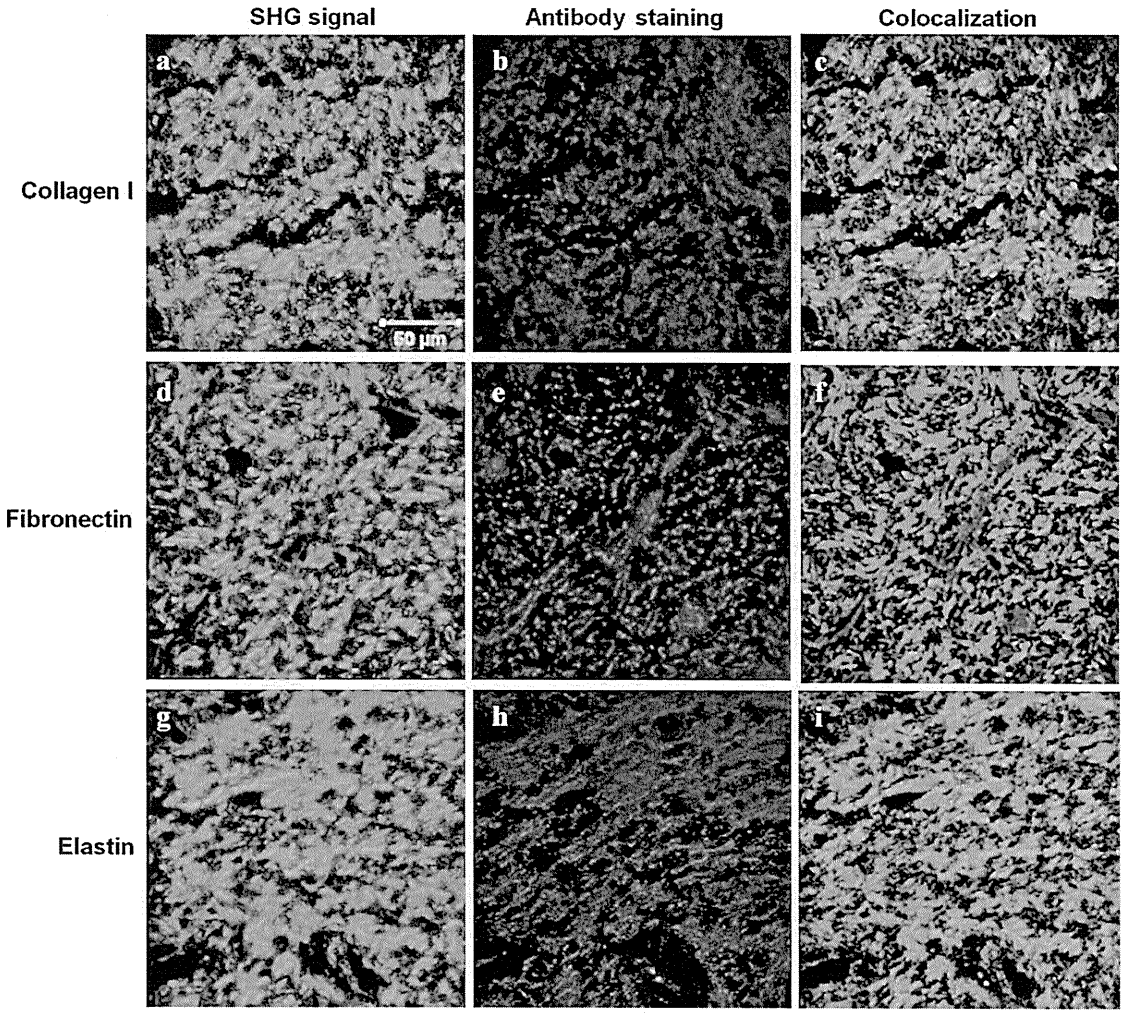

Fig. 1 – Co-localization of secondary harmonic image generation (SHG) and collagen I-, fibronectin- and elastin-antibody labeled human tissue sections show that the SHG signal closely co-localizes with collagen I-antibody staining, but not fibronectin or elastin. (a and d) SHG visualized on a frozen human *Normal* 1 tissue section, (g) SHG visualized on paraffin-embedded human *Normal* 1 tissue section, (b) collagen I-antibody labeled Alexa488 signal, (e) fibronectin-antibody labeled Alexa488 signal, (h) elastin-antibody labeled Alexa488 signal, and (c, f, and i) co-localization of SHG signal and antibody labeling.

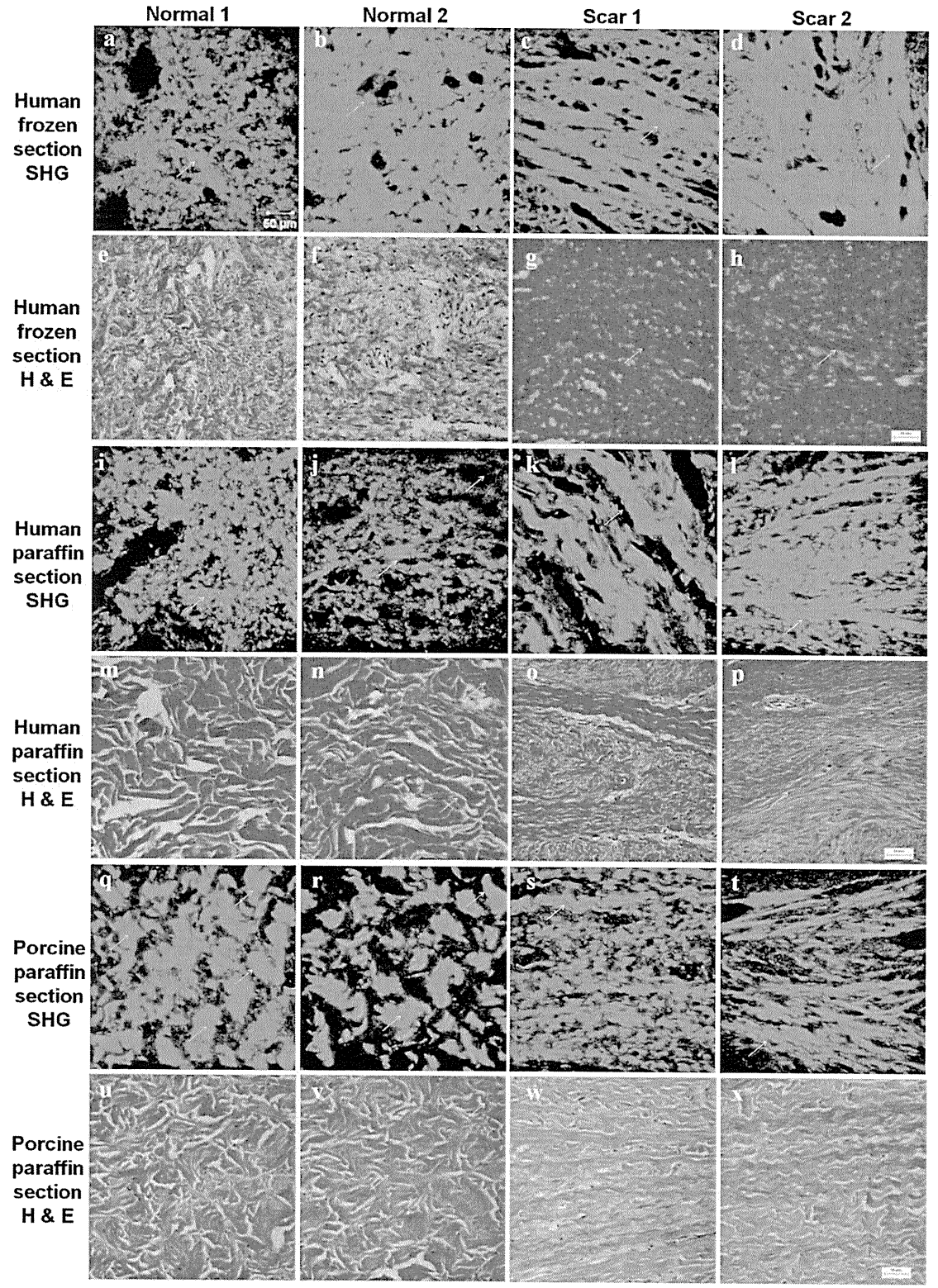

Fig. 2 – Human (a–p) and porcine skin (q–x) collagen architecture visualized using secondary harmonic image generation (SHG) and hematoxylin and eosin staining. All images were taken with the same microscope configuration/magnification to compare the differences in signal intensity and collagen arrangement between normal skin and scar tissue. The arrows in the control samples indicate the basket-weave arrangement in normal tissue, and highlight the elongated, wavy, undulating parallel collagen fibers observed in scar tissues. Collagen fiber bundles in H&E stained and SHG-visualized paraffin embedded sections

Cambridge, MA, USA) [20] or neat fibronectin supernatant monoclonal antibody HFN7.1 (DSHB, TX, USA) [21] at room temperature for 1 h in a humid atmosphere. After three washes in 0.1 M Dulbecco's phosphate buffered saline (PBS, five minutes per wash), slides were incubated in 1:500 Alexa Fluor 488 goat anti-mouse IgG antibody (Invitrogen, CA, USA) for 30 min at room temperature in a humid atmosphere in the dark. Microscope slides were washed three times in PBS, in distilled water and then coverslip mounted with Vectashield containing the nuclear staining agent, DAPI (1.5 μg/ml) (Vector Laboratories, Burlingame, CA, USA), and the coverslip edges sealed with non-fluorescent nail polish [22].

For elastin staining, as this antibody did not work in frozen sections, paraffin sections were dewaxed in xylene and processed through a descending ethanol series of washes, followed by trypsinization at 37 °C for 30 min using 0.2% trypsin (Gibco, CA, USA). Antibody permeabilization using 0.1% Triton X-100 (Merck, Australia) in PBS was performed at room temperature, incubated for 10 min with subsequent 30 min blocking in 10% normal goat serum (Millipore, CA, USA) in permeabilization solution at room temperature. Sections were incubated in 1:500 dilution monoclonal anti-elastin clone BA-4 (Sigma–Aldrich, MO, USA) [23] overnight at 4 °C. After three washes in PBS (five minutes each wash), slides were incubated in 1:500 Alexa Fluor 488 goat anti-mouse IgG antibody (Invitrogen, CA, USA) for 30 min at room temperature in the dark. Slides were then washed three times in PBS, then mounted with Vectashield with DAPI (Vector Laboratories, Burlingame, CA, USA) and the coverslips sealed with nail polish.

3. Results

To assess whether MPM is a viable alternative microscopic method to examine collagen deposition in control and burn scar tissues, we examined human normal skin and scar tissue using the MPM to detect SHG. Our results demonstrated that collagen SHG is best detected with lowest background noise at an excitation wavelength of 860 nm and an emission wavelength of 390–465 nm (data not shown). The localization of this putative collagen-SHG pattern was further compared to other dermal matrix components and was compared by dual channel colocalization with immunostaining using collagen I-, fibronectin- and elastin-antibody labeled tissue sections. The detected collagen-SHG signal showed a similar basket-weave arrangement pattern to collagen I antibody staining from normal human skin tissue (Fig. 1a and b), however the images did not completely overlap (Fig. 1c). Conversely, the putative collagen-SHG signal showed a completely different pattern when compared to fibronectin and elastin staining (Fig. 1f and i), with fibronectin demonstrating a finely organized nested pattern especially immediately below the epidermis (Fig. 1e), and elastin staining showed threads of thin fibers aligning in the same direction, parallel or perpendicular to the epidermis (Fig. 1h).

Two human control tissue samples and two human hypertrophic scar tissue samples were tested for SHG visualization and comparison with H&E staining at the optimal excitation wavelength of 860 nm, with an emission/collection wavelength of 390–465 nm. Collagen architecture in normal human dermis and burn hypertrophic scar tissue could be detected in both frozen (Fig. 2a–d) and paraffin sections (Fig. 2i–l) with similar signal intensity, however clearer collagen architecture was observed in the fixed paraffin-embedded sections (Fig. 2i–l). Collagen fibers in control foreskin sections were in a randomly but relatively loosely organized basket-weave-like arrangement, while scar tissue collagen fiber bundles comprised typically long fibers aligned in parallel or in an undulating pattern. Comparison with H&E stained cryostat and paraffin embedded sections confirmed the differences in collagen organization and packing observed by SHG between control and scar tissue. Comparison of H&E and SHG staining clearly demonstrated the higher density of collagen bundle packing in the scar samples in both cryostat (Fig. 2a–d versus e–h) and paraffin sections (Fig. 2i–l versus m–p). In general, SHG showed superior visualization of compacted collagen in bundles and the higher bundle density in human and porcine scar tissue compared to H&E stained sections. Furthermore, SHG provides significant improvements in collagen fiber resolution (see Fig. 2c and d, k and l, and s and t) that would allow clearer 3D image collection with the added benefit of ease of tissue preparation. Although the twisted or wavy characteristics of hypertrophic scar dermal collagen fibers were clearly observed in both scar sections, using both techniques (see arrows in Fig. 2k and o) no collagen nodules were visualized in these samples using either SHG or H&E visualization techniques.

The same approach was repeated using control porcine and hypertrophic scar paraffin-embedded sections to determine if different species exhibit similar optimal wavelengths for collagen SHG signal detection (see Fig. 2q–t). Our results show that porcine collagen SHG was best detected at excitation wavelength of 860 nm and an emission wavelength of 390–465 nm, which was identical to the detection of human dermal collagen (data not shown). Control porcine paraffin-embedded dermal tissue sections exhibited a stronger SHG signal intensity over the length of the shorter fibers (arrows in Fig. 2q and r) compared to scar tissue sections (Fig. 2s and t). Similar to human collagen architecture, control porcine dermis also demonstrated a basket-weave arrangement, while scar tissue exhibited extended, long wavy collagen fibers aligned in parallel with the epidermis (Fig. 2s and t). Again, H&E stained paraffin embedded sections confirmed the differences observed using SHG in collagen bundle distribution, length and packing between pig control and scar tissue samples.

exhibited identical distribution, length and packing patterns between human and porcine control and scar tissue samples. However, upon closer comparison SHG visualization exhibited increased resolution and clarity of individual collagen bundles, especially in scar tissue from all species examined (c and d, k and l, and s and t).